

Original article

Combination of non-ionic and cationic surfactants in generating stable CO₂ foam for enhanced oil recovery and carbon storage

Rishabh Tripathi¹, Zachary Paul Alcorn², Arne Graue², Sandeep D. Kulkarni¹✉*

¹Deysarkar Centre of Excellence in Petroleum Engineering, IIT Kharagpur, Kharagpur 721302, India

²Department of Physics and Technology, University of Bergen, Bergen 7800, Norway

Keywords:

Carbon dioxide geo-storage
CO₂ foam flooding
enhance oil recovery
carbon capture utilization and storage

Cited as:

Tripathi, R., Alcorn, Z. P., Graue, A., Kulkarni, S. D. Combination of non-ionic and cationic surfactants in generating stable CO₂ foam for enhanced oil recovery and carbon storage. *Advances in Geo-Energy Research*, 2024, 13(1): 42-55. <https://doi.org/10.46690/ager.2024.07.06>

Abstract:

Surfactant-stabilized CO₂ foam is a promising technology to reduce CO₂ mobility in geologic CO₂ storage and CO₂ enhanced oil recovery processes. In this study, various combinations of a non-ionic surfactant, Alkyl polyglycoside, along with cationic surfactants were ingeniously examined to enhance carbon storage and facilitate oil recovery through CO₂-based foam flooding. Specifically, for the first time, the investigation focused on the impact of altering the alkyl chain length and counter-ion type of the cationic surfactants. The surfactant combinations were first screened based on surfactant characterization, surface and interfacial tension studies and bulk foam experiments. The interfacial tension studies showed that, in combination with Alkyl polyglycosides, the C₁₆ (cetyltrimethylammonium bromide and cetyltrimethylammonium chloride) alkyl chain length cationic surfactants exhibited less interfacial tension values than the C₁₂ (dodecyltrimethylammonium bromide and dodecyltrimethylammonium chloride) alkyl chain length cationic surfactant. The bulk foam experiments established that Alkyl polyglycosides/C₁₆ combination showed higher foamability and foam stability than Alkyl polyglycosides/C₁₂ combination. The bulk foam investigation showed that the optimized concentration of Alkyl polyglycosides/cationic-surfactant was 0.3/0.15 wt%. The surfactant combinations screened from these studies were evaluated for EOR coreflooding experiments at 1250 psi and 60 °C. The incremental oil recovery obtained for baseline CO₂ and Alkyl polyglycosides/cetyltrimethylammonium bromide foam flooding was 18.5% and 32.7%, respectively. The estimated carbon storage potential for baseline CO₂ g and Alkyl polyglycosides/cetyltrimethylammonium bromide foam flooding was 11.9% and 23.7%, respectively. The combination of Alkyl polyglycosides cetyltrimethylammonium bromide surfactant was demonstrated as an effective solution for increased oil recovery and carbon storage.

1. Introduction

Large-scale subsurface CO₂ storage has become one of the attractive methods for reducing carbon emissions and achieving the limit of temperature rise under 2 °C (Wei et al., 2021). Matured oil and gas reservoirs are expected to have a capacity of 168 Gt for CO₂ storage using CO₂ enhance oil recovery (EOR) (Wei et al., 2021). Multiple large-scale commercial CO₂ storage projects like Sleipner and Weyburn have increased the knowledge and confidence in the

underground storage of CO₂ (Ma et al., 2022a). Four main mechanisms are associated with underground CO₂ storage in matured oil and gas reservoirs: Structural and/or stratigraphy trapping, residual or capillary trapping, solubility trapping, and mineral trapping (Adebayo, 2019). Different mechanisms associated with the underground storage of CO₂ in depleted oil and gas reservoirs are presented in Fig. 1. CO₂ flooding has been used primarily in the oil and gas industry as a part of EOR techniques. The growing importance of Carbon Capture Utilization and Storage has placed this category of

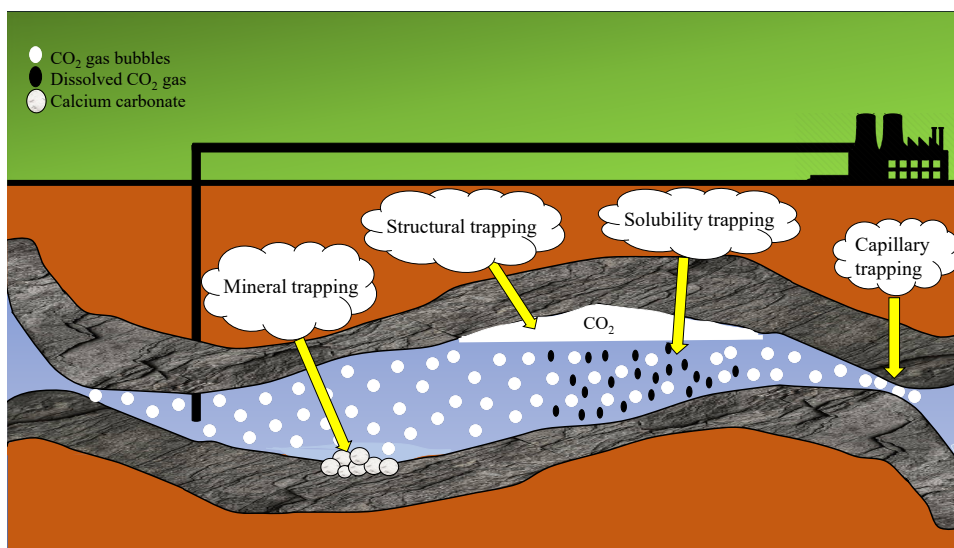


Fig. 1. Mechanisms associated with underground CO₂ storage in depleted oil and gas reservoirs.

EOR into the limelight. During the CO₂ EOR process, CO₂ is injected inside the oil reservoir either at miscible or immiscible conditions to produce the remaining oil present in the reservoir. The mobility of pure CO₂ is very high, resulting in early breakthroughs, reduced EOR and carbon storage potential. An important improvement in the CO₂ EOR technique was the use of CO₂ foam flooding instead of pure CO₂ flooding. Using CO₂ foam not only enhances the oil recovery but also increases the overall CO₂ storage potential inside the depleted oil and gas reservoir. CO₂ foam flooding mainly relies on structural and residual trapping mechanisms for underground CO₂ storage (Adebayo, 2019). Numerous field pilot projects have proved the potential of CO₂ foam flooding for enhancing oil recovery and carbon storage (Sanders et al., 2012; Alcorn et al., 2018). Screening of surfactants that can produce stable foams is an integral part of the design of foam flooding for effective CO₂ storage and oil recovery. A study performed by Pang and Mohanty (2023) studied different combinations of surfactants and nanoparticles for CO₂ foam flooding for enhanced oil recovery and CO₂ storage in carbonate reservoir. It was found that addition of nanoparticles in the non-ionic (Aspiro S 2410) surfactant solution increased the foam stability. The amount of CO₂ stored during foam flooding using only surfactant solution was less than the amount of CO₂ stored using nanoparticle stabilized surfactant generated CO₂ foam flooding. It was found that as the foam stability and foamability increases, the CO₂ storage increases. The CO₂ gas gets diverted into other less permeable areas of the reservoir due to the formation of stable CO₂ foams. It proves that the surfactants that can generate stable foams are of prime importance for increasing the CO₂ storage potential. One promising surfactant is the non-ionic Alkyl polyglycosides (APG), a biodegradable green surfactant. These surfactants are less toxic and highly biodegradable making them comparatively safe and environmentally friendly. Foams generated using APG surfactants are resistant to high temperatures and high salinity. In addition, quaternary ammonium salts have

been widely used as cationic surfactants for foam flooding applications. The quaternary ammonium compounds are a type of surfactant containing a positively charged nitrogen atom linked to 4 alkyl or aryl substituents. The water solubility of these surfactants depends on hydrophobic chain lengths and polarity. The literature has investigated APG and quaternary ammonium cationic surfactants for various scenarios of CO₂ foam flooding applications as summarized below.

Wei et al. (2018) studied the APG surfactants of different alkyl chain lengths, $n = 8.5$ to 10, 10.9, 12 and 12.9 for the CO₂ foam flooding application. The authors analyzed the foam flooding performance on the basis of surface tension characterization, bulk foam analysis, and core flooding experiments. The bulk foam analysis demonstrated optimum foam performance at APG ($n = 10$) which was supported by viscoelastic characterization of the surfactants of different alkyl chain lengths. The subsequent coreflooding experiment at 2,100 psi and 110 °C. for APG ($n = 10$) surfactant exhibited maximum apparent viscosity (0.015 Pa·s) at the CO₂ foam quality of 0.67. The APG surfactant generated foam flooding have also been applied for enhanced oil recovery applications and it has successfully been able to produce 13% incremental oil recovery at 50 °C temperature (Wu et al., 2024). The effect of pressure on the APG surfactant performance in terms of maximizing the CO₂ storage potential was investigated using the coreflooding experiments (Wen et al., 2024a). This study demonstrated maximum storage at pressure of 1,740 psi for the studied pressure range of (145, 1,740) psi. The impact of salinity on the APG surfactant performance was also investigated using the coreflooding experiments (Wen et al., 2024b). The authors demonstrated maximum apparent viscosity (0.06 Pa·s) across the core at the salinity of 200 gm/litre for the studied salinity variation of (50-200 gm/litre). The APG surfactants were studied in combination with the anionic surfactants. Wang et al. (2017b) screened various mixtures of APG-1214 and anionic surfactants using bulk CO₂ foam experiments. These authors demonstrated a synergistic

Table 1. The details of the related studies involving APG and cationic surfactants.

Authors	Surfactant	Experiments	Pressure (psi)	Temperature (°C)
Wei et al. (2018)	APG surfactants of different alkyl chain lengths, $n = 8.5, 10, 10.9, 12$ and 12.9 .	Surface tension bulk foam analysis core flooding experiments	2,103.05	110
Wu et al. (2024)	APG-0810	Foam Morphology and stability studies Mobility and apparent viscosity measurement Coreflooding experiments	1,740	25-50
Wen et al. (2024a)	APG-0810	MD simulations Coreflooding experiments	145-1,740	80
Wen et al. (2024b)	APG-0810	MD simulations Coreflooding experiments	1,450	79.85
Wang et al. (2017b)	APG-1214, SDS, NP, Sodium Dodecylbenzene Sulfonate	Coreflooding experiments	3,625	150
Thakore et al. (2021)	Alpha Olefin Sulphonate, Tergitol™ (NP-40), SDS, CTAC	Foamability and foam stability	400	200
Yu et al. (2021)	CTAC, DO, LO SP, CS	Surface tension core flooding experiments	2,000	90
Ma et al. (2022b)	CTAB, TTAB, DTAB	Bulk foam zeta potential particle size distribution surfactant adsorption	1,450	50

Notes: NP denotes Nonylphenol polyethoxylate.

effect of APG and sodium dodecyl sulfonate (SDS) surfactants i.e., when used in combination, the surfactant mixture was found to produce higher CO₂ foam volume as compared to that produced when either of the two surfactants were used alone. The bulk foam analysis was corroborated with the results of the flooding experiments using the surfactant mixtures of at 3,600 psi and 150 °C. The key parameters of the various literature studies on application of the APG surfactants for the CO₂ foam flooding are tabulated in Table 1.

The application of cationic surfactants for CO₂ foam flooding, especially in the limestone reservoirs, has been demonstrated by several researchers. Thakore et al. (2021) conducted bulk foam experiments using Cetyltrimethyl ammonium chloride (CTAC) for the applied pressure range of 100-400 psi at various temperatures ranging from 100 to 200 °C. These authors showed that the bulk foams half-life drastically reduced above 120 °C but increased significantly as the pressure was increased from 100 to 400 psi. Yu et al. (2021) compared performance of various cationic surfactants including Cetyltrimethyl ammonium chloride (CTAC), Decylamine Oxide (DO), Lauramine Oxide (LOSP) and Cocamidopropyl Hydroxysultaine (CS) surfactants. Based on CO₂ bulk foam experiments, these researchers ranked that performance of the studied cationic surfactants as: CS > CTAC > LO SP > DO. Further, the core flooding tests on the top two stable surfactants (CS and CTAC) demonstrated improved CO₂ storage potential at the conditions of 90 °C

and 2,000 psi. Another group of researchers Ma et al. (2022b) compared cationic surfactants (Tetradecyltrimethyl ammonium bromide (TTAB), cetyltrimethyl ammonium bromide (CTAB) and dodecyltrimethyl ammonium bromide (DTAB)) for the CO₂ foam flooding performance. On the basis of bulk foam experiments, these researchers demonstrated that the cationic surfactant with highest alkyl chain length (TTAB) showcased maximum foam stability at the studied conditions of 1,450 psi and 50 °C. The key parameters of the various literature studies on application of the cationic surfactants for the CO₂ foam flooding are tabulated in Table 1.

As the APG surfactants are environmentally friendly, it was imperative to study if a small addition of the cationic surfactants could lead to performance enhancement in terms of CO₂ storage and oil recovery enhancement. However, there are limited studies in the literature that indicated that a synergistic effect of the APG surfactant in combination with the cationic surfactants provided improved CO₂ storage and oil recovery (Wang et al., 2017a; Zhang et al., 2020). Additionally, these synergistic studies did not examine the effect of variation in alkyl chain length or counter-ion type of the cationic surfactants for optimizing CO₂ storage and improved oil recovery. To address this gap, the present work investigates the combination of APG with cationic surfactants (CTAB, CTAC, DTAB and dodecyltrimethyl ammonium chloride (DTAC)) having variation in both the alkyl chain length (C₁₂/C₁₆) and counter-ion type (chloride/bromide). The experiments included

Table 2. The details of cationic surfactants used for the study.

Surfactant	Type	Formula	Molecular weight	Cloud point (°C)
CTAB	Cationic	C ₁₉ H ₄₂ BrN	364.45	>120
CTAC	Cationic	C ₁₉ H ₄₂ NCl	320.00	>120
DTAB	Cationic	C ₁₅ H ₃₄ NBr	308.34	>120
DTAC	Cationic	C ₁₅ H ₃₄ ClN	263.89	>120

bulk foam studies, surface and interfacial tension studies, and oil recovery core flooding study, which would validate the surfactant formulation for maximizing CO₂ storage and oil recovery.

2. Materials and methodology

2.1 Materials

A combination of different cationic surfactants with non-ionic (APG) surfactants was used for the experiments. The cationic surfactants (Table 2) were CTAB, DTAB, CTAC and DTAC. The non-ionic surfactant, Alkyl polyglycoside (Triton CG-110), was used as purchased from Sigma Aldrich. The salts that were used to prepare the formation brine were certified ACS grade and commercially sourced. The composition of the formation brine and chalk brine is given in Table 3 (Jian et al., 2020). N-Decane (C₁₀H₂₂) was used as the oil phase has a density of 0.730 gm/cc at 15 °C. Nitrogen and carbon dioxide gas of purity >99.999% were used in the study.

Edwards limestone cores were used for the core flooding experiments. The size of the core was 6.58 (length, cm) × 3.75 (diameter, cm). The porosity and permeability was 17.5% and 26.7 mD, respectively. The composition of the Edwards limestone was determined using X-ray diffraction method. The physical and mineralogical properties of the core sample are given in Table 4. The X-ray diffraction data of the Edward limestone has been provided in supplementary material (Fig. S1).

2.2 Methodology

The methodology is presented in Fig. 2. Initially, surfactant characterization was performed, followed by the bulk foam studies, which determined the foamability and foam stability of different surfactant formulations. The concentration of the surfactants was screened using bulk foam studies. Interfacial tension measurements were performed further after bulk foam studies to establish the surfactant formulations interfacial behavior. Based on the results, the two top-performing surfactant formulations in terms of foam stability and foamability were tested in the core flooding experiments to find the amount of oil recovered and carbon dioxide storage potential. The procedure for each screening step is described below.

2.2.1 Surfactant characterization

The surface tension and critical micelle concentration (CMC) were determined for each surfactant solutions indi-

vidually using Biolin ThetaFlex Tensiometer at 25 °C and atmospheric pressure. Additionally, the surface tension of the non-ionic and cationic surfactant formulation was also measured at the concentrations based on the result produced using bulk foam equipment. In this study, the surface tension measurements were conducted in the air environment as it was reported that surface tension values remain unaffected by the type of surrounding gas i.e., air or CO₂ at the atmospheric pressure (Mohamed et al., 2010).

The cloud point was measured by placing 25 ml of 1 wt% concentration surfactant solution in a high-temperature resistant vial. The cloud point of the combination of nonionic and cationic surfactants was also inspected at the concentration based on the result produced using bulk foam equipment. The sample was kept in the heating cabinet at 60 °C for 6 hours. After every hour, the solution was inspected for cloud point, and the volume of the solution was again measured to ensure there was no loss of solution. The process was repeated for temperatures up to 120 °C. None of the surfactants showed any cloudiness at 1 wt% concentration till 120 °C up to 6 hours. All the surfactants were thermally stable.

2.2.2 Bulk foamability and foam stability

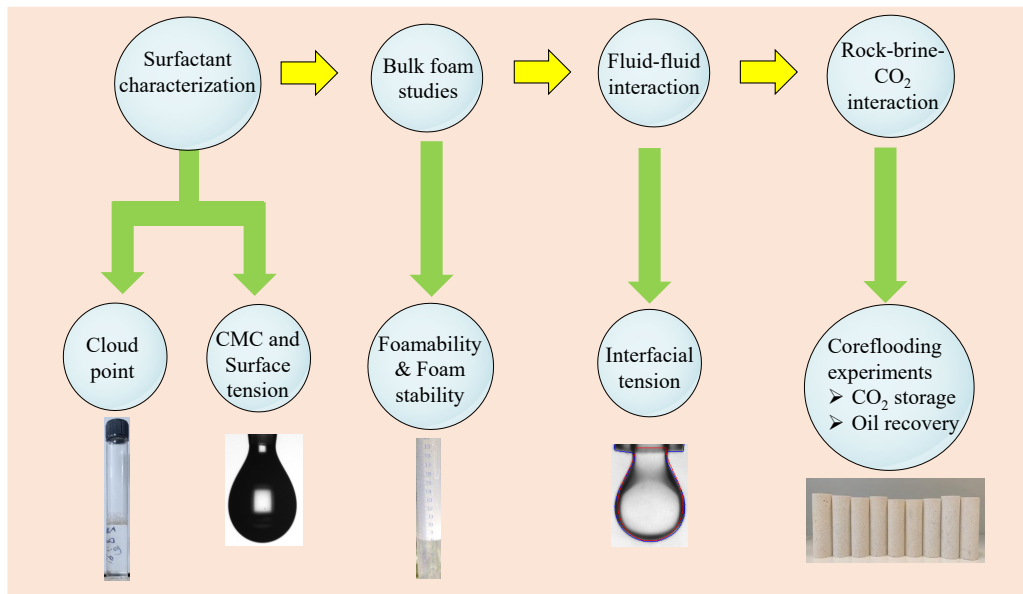
The bulk foam studies were conducted to quantify initial height (foamability) and half-life (foam stability). The bulk foam experimental setup consists of a foam generator with a 50.0 cm long glass chromatography column with an I.D. of 2.0 cm and 0.3 cm thick porous frit with a 40-100 μm pore size. The porous frit was placed to cause gas sparging in the surfactant solutions. Initially, 25 ml of surfactant solution was poured into the chromatographic glass column, and it was heated in the heating cabinet where the temperature was set at 60 °C respectively. A constant volumetric flow of 20 ml/min of N₂ gas was injected into the glass column for 5 min using a mass flow controller for foam formation. The initial foam height and subsequent decay (up to 600 seconds) were recorded using a high-resolution camera for each surfactant combination. The complete schematic of the bulk foam setup used for the study is presented in Fig. 3. Experiments were repeated three times to ensure consistency. The studied concentrations of the APG and cationic surfactant formulations are presented in Table 5.

2.2.3 Interfacial tension measurement

The interfacial tension was measured by producing a droplet of surfactant solution in the presence of n-Decane at 25 °C and atmospheric pressure. Interfacial tension between APG surfactant and n-Decane is independent of temperature between 25 and 60 °C (Kutschmann et al., 1995). Therefore, the data generated at the room temperature may reasonably reflect the qualitative comparison of the studied surfactant combinations. The image of the produced droplet was captured by Biolin Thetaflex Tensiometer, and it was processed using the ImageJ software pendant drop plugin (Daerr and Mogne, 2016). Three data values were processed, and the average values were stated along with the error.

Table 3. The composition of the formation brine and chalk brine used for the study.

Formation brine		Chalk brine	
Name	Composition (gm/ltr)	Name	Composition (gm/ltr)
NaCl	29.26	NaCl	50
MgCl ₂ ·6H ₂ O	2.76	CaCl ₂ ·2H ₂ O	50
CaCl ₂ ·2H ₂ O	5.82	Total dissolved solids (ppm)	100,000
KCl	0.46	pH	6.04
Total dissolved solids (ppm)	38,300	Density at NTP (gm/cc)	1.05
pH	9.71	Viscosity (cp)	1.09
Density at NTP (gm/cc)	1.014		

**Fig. 2.** The methodology followed in the present study to screen out the composition of non-ionic and cationic surfactants for foam flooding.**Table 4.** The physical properties and mineralogical composition of the Edward Limestone cores.

Properties	Values
Length (cm)	6.58
Diameter (cm)	3.75
Porosity (cm ³)	12.68
Permeability (mD)	26.7
Calcite (wt%)	98.9
Other minerals (wt%)	1.1

Table 5. The concentration of nonionic and cationic surfactant formulations for bulk foam study.

Surfactants	Conc. 1 (wt%)	Conc. 2 (wt%)	Conc. 3 (wt%)	Conc. 4 (wt%)
APG	0.1	0.2	0.3	0.4
APG/CTAB	0.1/0.05	0.2/ 0.1	0.3/0.15	0.4/0.2
APG/DTAB	0.1/0.05	0.2/ 0.1	0.3/0.15	0.4/0.2
APG/CTAC	0.1/0.05	0.2/ 0.1	0.3/0.15	0.4/0.2
APG/DTAC	0.1/0.05	0.2/ 0.1	0.3/0.15	0.4/0.2

2.2.4 Core flooding experiments

Alternate injection of CO₂ gas and surfactant formulations was performed to study foam generation, enhanced oil recovery, and associated CO₂ storage potential for the surfactant formulations (APG/CTAC and APG/CTAB) screened from the

earlier experiments. The schematic of the core flooding setup is illustrated in Fig. 4. The core flooding setup was pressurized to 1,250 psi at a temperature of 60 °C. The core plugs were covered with Teflon tape to minimize the radial CO₂ diffusion into the surrounding Viton rubber sleeve. The cores were placed inside a horizontally positioned biaxial hassler core

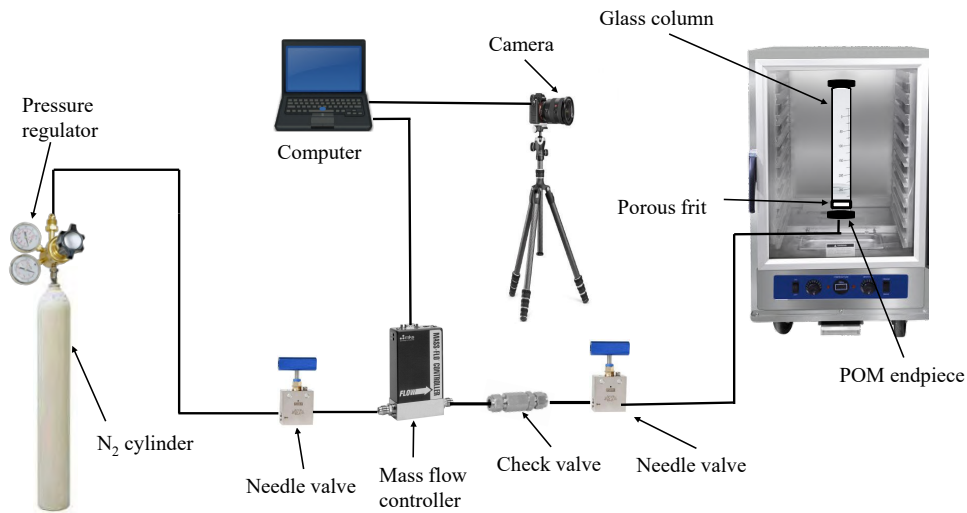


Fig. 3. Schematic diagram of the bulk foam setup used for measuring foamability and foam stability of surfactant formulations.

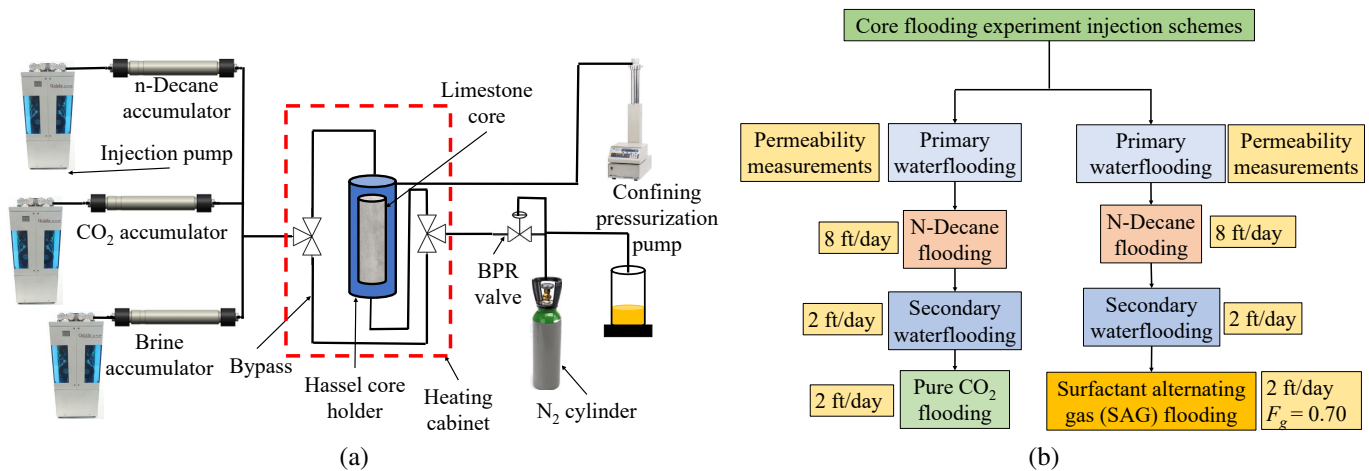


Fig. 4. Schematic diagram of (a) the core flooding setup used for measuring oil recovery and carbon storage (b) The injection scheme that was followed for the core-flooding experiments.

holder. The ISCO pump was used to provide the confinement pressure. The overburden pressure that was applied over the core was 2,300 psi. The pressure of the system was maintained using one Equilibar backpressure regulator. The fluids were injected using Quizix pumps (see Fig. 4(a)). Two pressure transducers and a differential pressure transducer were used to measure and control the pressure response.

The synthetic oil, n-Decane was shown to provide more destructive effect on generated foams as compared to reservoir crude oil (Razavi et al., 2020). Therefore, using n-Decane instead of crude oil might be the worst-case scenario for the production of in-situ foam. Accordingly, n-Decane was used to simulate the oil phase for the coreflooding experiment at the reservoir pressure and temperature. The injection scheme for core-flooding experiments is given in Fig. 4(b). Each core flooding experiment started with initially measuring permeability using chalk brine Table 3, followed by primary drainage in which the n-Decane was injected into the core at a rate of 8 ft/day (1.87 cc/min). Secondary waterflooding

was performed by injecting chalk brine at a rate of 2 ft/day (0.47 cc/min) to mimic the secondary recovery technique, until there was no oil production. Finally, foam flooding was performed for each surfactant formulation using an alternating injection sequence of surfactant and supercritical CO₂. Nine such surfactant-alternating-gas (SAG) cycles were performed for each surfactant formulation. Due to the challenges of well injectivity, co-injection of CO₂ and surfactant solution may be impracticable at field scale; therefore, a SAG test in the core-flooding apparatus mimics the field application better than a co-injection test. In the present study, each SAG cycle consisted of a 30% (v/v) surfactant solution slug followed by a 70% (v/v) CO₂ slug (foam quality: 70%) constitute to an overall volume of 0.6 pore volume (PV). The selection of the slug size was based on the previous literature which demonstrated that the experimental oil recovery obtained from the core flooding apparatus was independent of the slug size for the studied range of parameters (Ding et al., 2022). The surfactant solution and gas were injected at a rate of 2

ft/day (0.47 cc/min). After each core flooding experiment, the same core was cleaned with the isopropanol solution until a clear solution was obtained from the outlet side. The EOR coreflooding experiments were performed at a pressure of 1,250 psi and a temperature of 60 °C. Under this condition, the CO₂ would become supercritical, but its density would remain comparable to gas ≈ 0.3 g/cc (Onyebuchi et al., 2018). It was also noted that the minimum miscibility pressure of CO₂ for n-Decane at 60 °C temperature was reported as 1,500 psi (Kian and Scurto, 2018). Thus, immiscible supercritical CO₂ foam flooding for the screened surfactant formulation has been explored in this work. The produced fluids were depressurized and collected in a glass cylinder, and CO₂ gas was vented out through an adsorption column. The mass and volume of the liquids produced were used for material balance to calculate the fluid saturation for estimating the CO₂ stored in the limestone core. CO₂ storage capacity is defined as the portion of pore volume that is available for CO₂ storage. The potential of carbon dioxide stored during the core flooding experiment was calculated using the following Eq (1):

$$\text{CSP}(\%) = \frac{V_1 + V_2 - V_3}{V_p} \times 100\% \quad (1)$$

where CSP (%) is the carbon storage potential, V_1 is the volume of oil produced, V_2 is the volume of water produced, V_3 is the volume of water injected, and V_p is pore volume. This estimation did not include the amount of CO₂ dissolved in the water and oil phases.

3. Results and discussion

3.1 Surfactant characterization

The CMC is the minimum surfactant concentration above which no further decrease in the surface tension is observed. The surface tension becomes constant above CMC (σ_{CMC}). The CMC of the studied surfactants in the brine solution is presented in Fig. 5, the x -axis is the surfactant concentration (wt%) presented in a logarithmic scale, and the y -axis is the surface tension measured in mN/m. The study demonstrated that, for the investigated cationic surfactants, the CMC and (σ_{CMC}) of high alkyl chain length surfactants (C_{16}) was lesser than that for the low alkyl chain length surfactant (C_{12}), e.g. CMC and (σ_{CMC}) of CTAB solution was ≈ 0.02 wt% (5.48×10^{-4} M) and 34.46 mN/m respectively whereas that for DTAB solution was ≈ 0.04 wt% (1.29×10^{-3} M) and 37.59 mN/m respectively. The observed variation with alkyl chain length agreed with the respective values reported in the literature, which may be explained on the basis of increased hydrophobicity of higher alkyl chain length CTAB and CTAC surfactants (Zhang et al., 2017). Fig. 5 also illustrated that the surface tension readings were affected by the counter-ion effect between Br⁻ ions and Cl⁻ ions for C_{16} and C_{12} surfactant solutions. The Br⁻ ions of CTAB and DTAB solutions provide higher attraction towards the micelle surface, reducing the surface charge as compared to the Cl⁻ ions CTAC and/or DTAC, leading to lower CMC values in the bromide-based surfactant solutions (Para et al., 2006). It was reported that for the non-ionic APG surfactant solution, the CMC value \approx

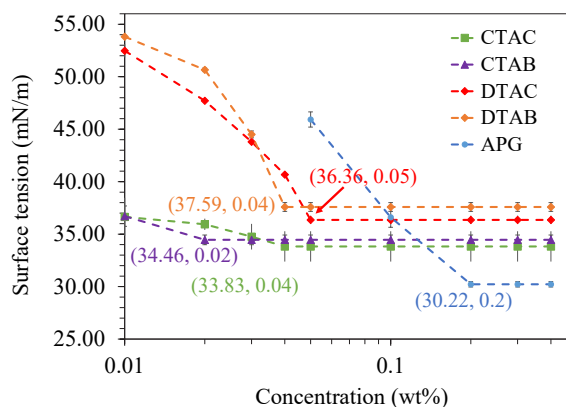


Fig. 5. The CMC of individual non-ionic (APG) and cationic surfactants (CTAC/CTAB/DTAC/DTAB) by measuring surface tension.

0.2 wt% (6.24×10^{-3} M) was order of magnitude higher than the studied cationic surfactants (Fig. 5). The non-ionic APG surfactant also provided a minimum (σ_{CMC}) of 30.22 mN/m. The CMC of APG surfactant in pure water was reported at 3.7×10^{-4} M with a surface tension of 39.73 mN/m (Chai et al., 2018).

3.2 Bulk foam studies

The experimental bulk foam studies were conducted by injecting the gas at a specified volumetric flow rate through various surfactant solutions (Section 2.2.1) at 60 °C. After the injection process of five minutes, the initial bulk foam volume (foamability) and foam decay response as a function of time were determined. For this study, the ratio of non-ionic (APG) and cationic surfactants was chosen to be 2 : 1 based on the optimization studies conducted in the literature (Zhang et al., 2020).

Fig. 6 illustrates that the order of foamability for different surfactant formulations is as follows: APG/CTAC > APG/CTAB > APG > APG/DTAC > APG/DTAB. This order of foamability was found to be consistent at all of the surfactant concentrations. The data established that the high alkyl chain length surfactants (C_{16}) demonstrated higher foamability than the low alkyl chain length surfactant (C_{12}) owing to the increased adsorption energy of CTAB and/or CTAC as compared to DTAB and/or DTAC (Petkova et al., 2020). The concentrations of surfactants were higher than the individual CMC of the surfactants, as the micellization/de-micellization was reported to aid foamability (Patist et al., 2001). It was noted in the present work that the foamability reaches the peak values at a concentration of 0.3/0.15 wt% of APG/cationic surfactant for all the cationic surfactants (Fig. 6). For example, in the case of the APG/CTAC surfactant combination, the foamability was increased from 78.1 to 106.6 cc as the surfactant concentration was raised from 0.1/0.05 to 0.3/0.15 wt%; further rise in the surfactant concentration did not aid foamability (Fig. 6). APG surfactant's foamability supersedes the foamability of APG/DTAB and APG/DTAC. The APG surfactants are non-ionic surfactants that dissolve in solution through hydrogen bonding. Adding salts increases the stability

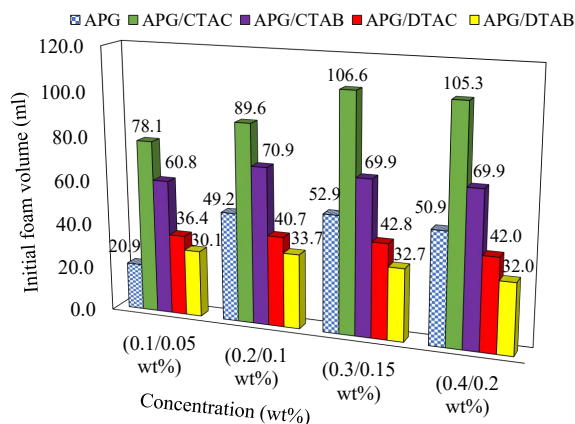


Fig. 6. Foamability of various combinations of non-ionic/cationic surfactants at different concentrations under a constant temperature environment ($T=60\text{ }^{\circ}\text{C}$).

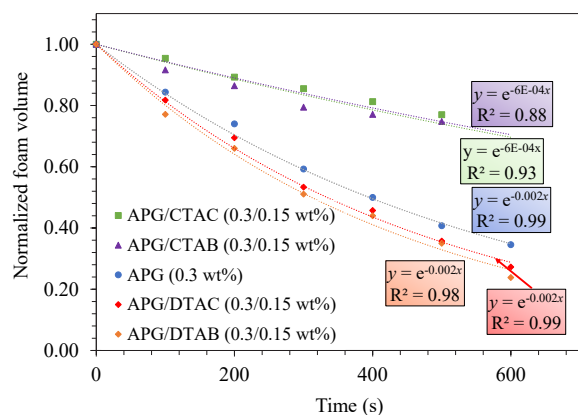


Fig. 7. Normalized foam decay of different combinations of non-ionic and cationic surfactants (0.3/0.15 wt%) at $60\text{ }^{\circ}\text{C}$. The standard deviation for the experiment was 0.06.

of APG surfactant in the foam film in the following order: $\text{Mg}^{2+} > \text{Ca}^{2+} > \text{Na}^{+}$. The cations head near the hydration layer around the surfactant head. The attraction between the cations and hydration layer reduces the diffusion coefficient of water molecules, enhancing foam lamellae’s water holding capacity. This increases the foamability and foam stability of the foam generated using APG surfactant (Xiao et al., 2022). The combined effect of decreased surface adsorption capability and hydrophobicity of DTAB and/or DTAC surfactants when compared to CTAB and/or CTAC surfactants caused foamability of APG to be higher than the combination of APG/DTAB and APG/DTAC surfactant formulations (Patist et al., 2001; Chai et al., 2018; Petkova et al., 2020).

The understanding of foam decay with time illustrates the stability of the foam which is known to impact EOR and carbon storage efficiency. Fig. 7 demonstrated the time dynamic of normalized foam volume for different surfactant formulations investigated for the optimized concentration of 0.3/0.15 wt% of APG/cationic surfactant at $60\text{ }^{\circ}\text{C}$. The degradation of foams with respect to time was modeled using first-order kinetics as stated below:

$$y = y_0 e^{-kt} \quad (2)$$

where y is the normalized height of foams at a particular time t , y_0 is the initial normalized height of foam at time 0 ($y_0 = 1$), k is the rate constant of the first order kinetics, and t is the time. The high values R^2 ($R^2 > 0.90$) for the modeled decay response underline the applicability of first-order kinetics, which was in agreement with earlier studies of foam kinetics for anionic and cationic surfactants (Thakore et al., 2021). Fig. 7 demonstrates the novelty of the present work in terms of comparing half-life ($t^{1/2}$) for studied combinations of APG with the cationic surfactants. Accordingly, the decreasing order of foam stability was as follows: $\text{APG/CTAC} \approx \text{APG/CTAB} > \text{APG} \approx \text{APG/DTAC} \approx \text{APG/DTAB}$. The data established that the studied high alkyl chain length surfactants (C_{16}) demonstrated higher foam stability than the low alkyl chain length surfactant (C_{12}) combined with the APG surfactant. The foam half-life ($t^{1/2}$) of APG/CTAC and APG/CTAB surfactant combinations was approximately 1,200 seconds, whereas the foam half-life of APG, APG/DTAC, and APG/DTAB were significantly lower ($t^{1/2} \approx 320\text{-}400$ seconds). This prominently higher foam stability of APG and C_{16} cationic surfactant combinations was one of the critical results demonstrated by the present study. The fundamental behavior was explained on the basis of higher surface adsorption and electrostatic repulsion caused by electrical double layer (EDL) interactions for the C_{16} cationic surfactant combined with APG; the proposed mechanism is illustrated in Fig. 8. The earlier literature presented the bulk foam studies under various experimental conditions; however, these studies did not address the impact of alkyl chain length on a combination of APG and cationic surfactants. Li et al. (2021) reported the foaming ability of CTAB surfactant using the Ross-miles method for bulk foaming experiments. It was noted that the CTAB surfactant exhibited a constant foaming ability above 0.1 wt%. Wei et al. (2022) performed bulk foam experiments using 0.1 wt% APG surfactant, the foam generated decayed exponentially with $t^{1/2} \approx 500$ seconds at room temperature. Wang et al. (2017b) conducted the bulk foam experiments using the warring blender method and it demonstrated that the maximum foamability and foam stability were obtained for APG surfactants at 0.3 wt% concentration. The 0.1 wt% of DTAB surfactant generated foam using CO_2 gas, the $t^{1/2} \approx 100$ seconds (de Azevedo et al., 2023). The comparison of the literature data with our work suggests that the combination of APG with C_{16} cationic surfactant maximized the foamability and foam stability, as illustrated in the present study.

3.3 Surface tension and interfacial tension

The earlier bulk-foam studies (Section 3.2) demonstrated that the optimum foamability response was obtained at a concentration of 0.3/0.15 wt% of the APG/cationic surfactant for the studied surfactant combinations. Accordingly, surface and interfacial tension studies were carried out under this optimized condition. Table 6 demonstrated that surface tension values for the optimal combination of APG and cationic sur-

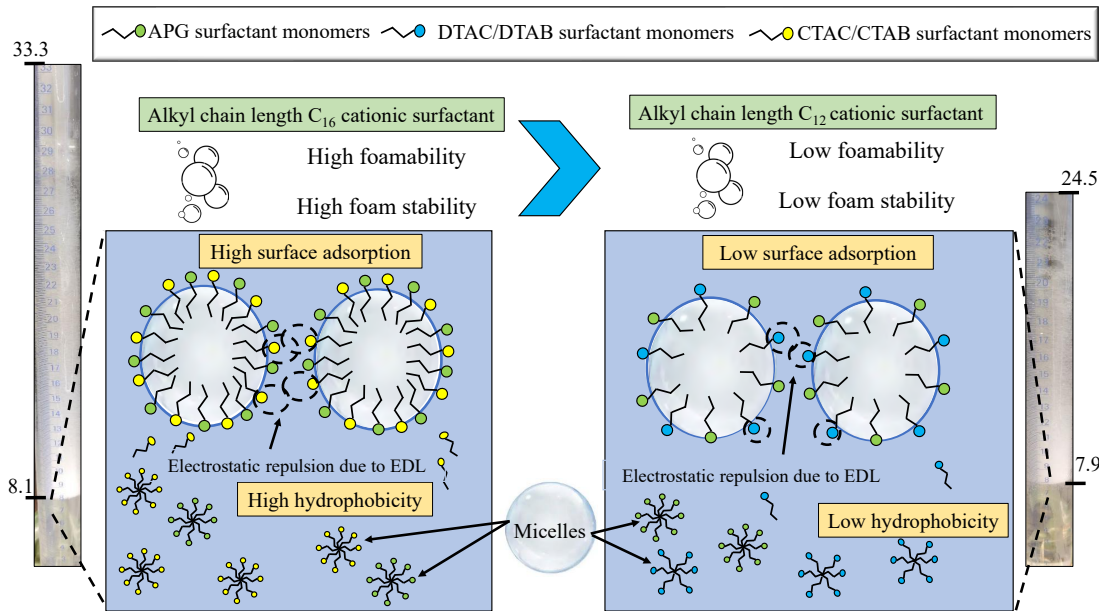


Fig. 8. The difference between the foamability and foam stability of alkyl C_{16} and C_{12} chain lengths cationic surfactants when used in synergy with APG surfactant.

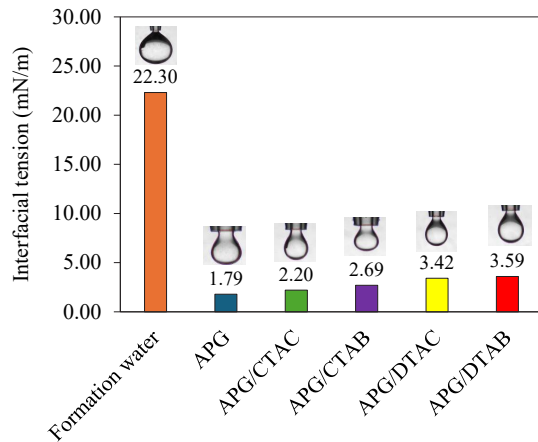


Fig. 9. Interfacial tension studies for the non-ionic surfactants (0.3 wt%) and cationic surfactants (0.15 wt%) at 25 °C and n-Decane. The error % for the experiment was 0.51.






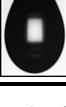
factants were in decreasing order as follows: APG/DTAB > APG/DTAC > APG/CTAB > APG/CTAC > APG. Fig. 9 showcased interfacial tension value for the optimal combination of APG and cationic surfactants in the presence of the synthetic oil (i.e., n-Decane); this investigation shall be relevant to provide a microscopic understanding of the core flooding experiments (illustrated in the following section) that were performed in the presence of n-Decane. The investigation demonstrated that interfacial tension values for the studied combination of APG and cationic surfactants followed the same trend as their surface tension behavior: APG/DTAB > APG/DTAC > APG/CTAB > APG/CTAC > APG. The stand-alone APG surfactant formulation obtained the lowest interfacial tension value at 1.79 mN/m. The literature studies at varied salinities had provided interfacial tension values of the stand-alone surfactants in the presence of n-Decane as

follows: APG (0810)-1.18 mN/m; DTAB-2.94 mN/m; CTAB-1.75 mN/m; which may form the basis of the observed trend for interfacial values of surfactant combinations in the present work (Santa et al., 2011; Yekeen et al., 2019; Chen et al., 2022). As the hydrophobic chain length increases, the interfacial tension between the surfactant formulation and synthetic oil is expected to decrease. It may explain cetyl-based (C_{16}) surfactants exhibiting less interfacial tension values than dodecyl-based (C_{12}) surfactants. The APG surfactant, being non-ionic, showed the lowest interfacial tension as more number of surfactant molecules could accumulate at the interface in the absence of surface charge (Santa et al., 2011).

3.4 Core flooding experiments

The EOR core flooding experiments quantified enhanced CO_2 storage and oil recovery with in-situ foam formation using the above selected surfactant formulations. The core flooding experiments were performed for APG and C_{16} cationic surfactant (CTAB/CTAC) combinations because they provided maximum foam-stability and minimal interfacial tension values (Sections 3.2 and 3.3). Additionally, this core flooding study was performed at the optimal concentration of 0.3/0.15 wt% of the APG/cationic surfactant based on the outcome of the bulk foam studies discussed in Section 3.2. The differential pressure across the core during secondary waterflooding was stabilized to ≈ 11.0 psi, leading to an oil recovery of $\approx 35.5\%$. Following the waterflooding process, alternating injection of the surfactant formulation and CO_2 began in cycles to induce in-situ foam generation (termed CO_2 foam flooding). The dynamic differential pressure (psi) values measured across the core during these SAG cycles are shown in Figs. 10(a) and 10(b). The differential pressure response was also compared with that of the baseline CO_2 flooding shown in Fig. 10(c). The pressure data was used to determine

Table 6. The surface tension of different surfactant formulations screened from bulk foam study.

Surfactant	Concentration (wt%)	^a Surface tension	Captured image	^a pH	Cloud point (°C)
Formation brine	See Table 3	69.40 ± 2.55		9.71	/
APG/CTAC	0.3/0.15	30.09 ± 1.11		8.05	> 120
APG/CTAB	0.3/0.15	30.98 ± 1.14		7.81	> 120
APG	0.3	30.04 ± 1.10		9.55	> 120
APG/DTAC	0.3/0.15	31.36 ± 1.15		7.81	> 120
APG/DTAB	0.3/0.15	31.43 ± 1.15		7.97	> 120

Notes: ^aSurface tension, cloud point and pH were determined in the formation brine.

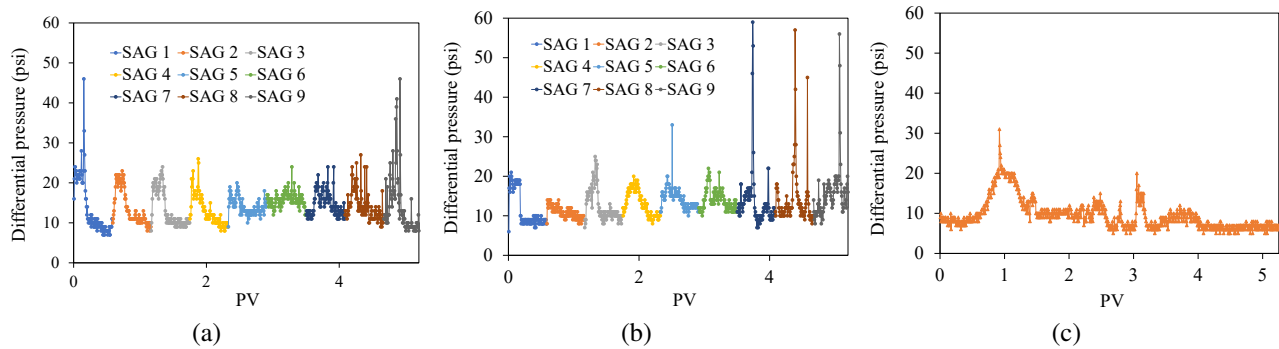


Fig. 10. The dynamic differential pressure values (psi) measured across the core during the EOR core flooding experiments for (a) 0.3/0.15 wt% of APG/CTAB surfactant formulation, (b) 0.3/0.15 wt% of APG/CTAC surfactant formulation and (c) baseline CO₂ flooding with respect to the PV injection.

the apparent viscosity of the in-situ generated foams during application of the two studied surfactant combinations based on the following equation (Ding et al., 2022):

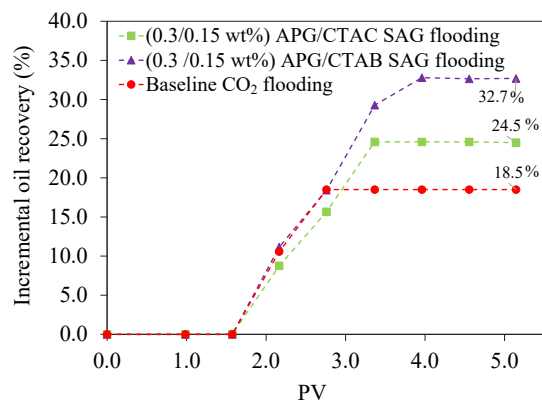
$$\mu_{foam} = \frac{KA\Delta P_{avg}}{L(Q_g + Q_L)} \quad (3)$$

where K is the permeability of the core, Q_g and Q_L is the gas and liquid injection rate, A is the area of the core core-section, ΔP_{avg} is the average differential pressure along the core during foam flooding, μ_{foam} is the apparent viscosity and L is the length of the core. Based on this formula, the apparent viscosity of baseline CO₂ flooding was 0.0016 Pa-s. The calculated apparent viscosity of the APG/CTAB and APG/CTAC foam flooding were reported to be 0.0025

and 0.0024 Pa-s, respectively. Similar viscosity values were reported in the literature for APG surfactant-based CO₂ foam using a viscometer under applied pressure of 1,450 psi at room temperature in the absence of crude oil (Wu et al., 2021). Although the CO₂ foam flooding resulted in higher apparent fluid viscosity than baseline CO₂ flooding, it was noted that the viscosity values were lower compared to that reported for the N₂ foam flooding in the literature. For instance, Ding et al. (2022) investigated the co-injection of 0.5 wt% APG surfactant solution and nitrogen gas into a 75 mD limestone core at a pressure of 1,450 psi and 55 °C. These authors noted an apparent viscosity of 0.010 Pa-s for the foams generated in-situ in the presence of crude oil. The foams generated using CO₂ are weaker than that generated using N₂ gas owing to hi-

Table 7. Oil recovery and CO₂ storage potential during core flooding experiments at 1,250 psi and 60 °C.

Surfactant injection	Initial oil in place (%)	Water-flooding (%)	Incremental CO ₂ SAG foam flooding (%)	Carbon storage potential (%)
APG/CTAB	≈ 67.5%	≈ 35.5%	32.7%	23.7%
APG/CTAC	≈ 67.5%	≈ 35.5%	24.5%	15.8%
CO ₂ flooding	≈ 67.5%	≈ 35.5%	18.5%	11.9%

**Fig. 11.** The incremental oil recovery values against injected PVs through the core for APG/CTAB foam flooding (0.3/0.15 wt%), APG/CTAC foam flooding (0.3/0.15 wt%) and the baseline CO₂ flooding during the coreflooding experiments.

gher solubility of CO₂ in water and generation of carbonic acid upon dissolution in water (Bello et al., 2022).

There was a considerable improvement in incremental oil recovery and carbon storage potential for the CO₂ foam flooding in the current experiment, which could be correlated with the higher apparent viscosity values and lower interfacial tension values compared to the baseline CO₂ flooding. The rise in the incremental oil recovery with respect to the injected PV fluid injected for the different flooding scenarios was demonstrated in Fig. 11. The similar initial response of the incremental recovery vs. PV injection for both the foam and gas flooding scenarios (up to 2.5 PV) were corroborated with reported experimental as well as simulation studies on foam/gas flooding using various surfactants (Sæle et al., 2022). However, it was noted that, once the oil recovery tends to reach to a plateau (≈ 3.0 PV fluid injection), the ultimate recovery for foam flooding was considerably higher compared to the baseline gas flooding (Fig. 11). The ultimate incremental oil recovery obtained for APG/CTAC and APG/CTAB based foam flooding was 24.5% and 32.7%, respectively (Table 7). On the contrary, the baseline CO₂ flooding yielded only 18.5% incremental oil recovery. Similar enhanced oil recovery values for standalone CTAB foam flooding were reported by Massarweh and Abushaikha (2023) as the oil recovery neared the saturation.

The CSP (%) in the rock core during the coreflooding experiments was estimated using Eq. (1) and the results are

presented in Table 7. The measured amount of CO₂ stored in the core sample during the experiments of APG/CTAC and APG/CTAB based CO₂ foam flooding was 15.8% and 23.7%, respectively, which was significantly higher than that measured for baseline CO₂ flooding (11.9%). The foam flooding would lead to improved displacement in the rock pores (compared to baseline CO₂ flooding) which resulted in higher oil recovery as well as enhanced CO₂ storage; as consistently observed in these core flooding experiments (Table 7). It was concluded that the foam flooding enhanced the overall oil recovery and underground carbon dioxide storage potential, which underlines the importance of foam stability and foamability studies as screening criteria for surfactant formulations. Despite having comparable differential pressure for the two studied foam flooding scenarios, the APG/CTAB based foam-flooding provided a higher incremental oil recovery and CO₂ storage potential when equated with the APG/CTAC based foam-flooding. One possible reason for this behavior would be the wettability alteration from oil-wet to water-wet, caused by the more effective counter-ion effect: Br⁻ vs. Cl⁻ (Hou et al., 2022).

The reported literature corroborated the advantage of foam flooding. For instance, Rezaee et al. (2022) and demonstrated improved recovery for heavy oil displacement, albeit in the case of N₂-based foam flooding (co-injection and SAG scenarios) using stand-alone CTAB surfactants at temperatures up to 80 °C. The literature studies for foam flooding using stand-alone APG surfactants included the investigation using 0.2-1.0 wt% APG surfactant solution at 55 °C and 1,450 psi pressure (Ding et al., 2022). The improved oil recovered during foam flooding of 0.5 wt% APG surfactant solution using the co-injection technique was 10.3%. Rafati et al. (2012) performed coreflooding experiments and found that 1 wt% of APG surfactant solution generated foam flooding produced 56% overall oil recovery. In his study, paraffin oil of 0.85 gm/cc density was used as an oil phase. The amount of CO₂ was stored for APG in the absence of crude oil at the pressure and temperature of 1,450 psi and 80 °C was 54.17% (Wen et al., 2024a). Compared to the results from the current study, the destructive effect of n-Decane on foam stability, decreases the overall CO₂ storage potential for foam flooding. The amount of CO₂ storage potential for the non-ionic surfactant generated foam flooding (Aspiro S 2410) at the pressure and temperature of 1,910 psi and 63 °C was 20.2% (Pang and Mohanty, 2023). In the same study, addition of silica nanoparticle in the non-ionic surfactant exhibited higher CO₂ storage of 30.7%. Baseline CO₂ flood studies without foaming solutions have reported poor improved oil recovery (< 8%) and meager CO₂ storage potential (< 10%) (Sæle et al., 2022). The early gas breakthrough and the significant difference in mobility between oil and gas were the prominent reasons for poor oil recovery and carbon storage during CO₂ flooding performed after waterflooding. The literature investigation along with the data reported in the present work established that the APG/CTAC and APG/CTAB surfactant formulations were more effective than standalone APG in enhancing the oil production and carbon dioxide storage potential in the limestone reservoirs.

4. Conclusions

In order to improve the incremental oil recovery and carbon storage potential in the limestone reservoirs, various combinations of APG and cationic surfactants were investigated in this work. The first part of the work included screening different combination of APG and cationic surfactant formulations using bulk foam experiments, surface tension and interfacial tension studies. The primary goal of the investigation was to identify the optimal surfactant combination by quantitatively estimating the amount of incremental oil recovery and carbon storage potential, supported by the screening studies. The cationic surfactants that were examined in the study vary in alkyl chain length and counter-ion type; these variations were studied for the first time in combination with the APG surfactant. The quantitative estimate of the enhanced oil recovery and carbon storage were determined using core flooding experiments at reservoir temperature (60 °C) and pressure 1,250 psi. The following results were obtained from the experiments:

- 1) Based on the bulk foam experiments, the order of foamability for different surfactant formulations were as follows: APG/CTAC > APG/CTAB > APG > APG/DTAC > APG/DTAB. The decreasing order of foam stability was as follows: APG/CTAC \approx APG/CTAB > APG \approx APG/DTAC \approx APG/DTAB. The optimized concentration of 0.3/0.15 wt% of APG/cationic surfactant were established from the bulk foam experiments at 60 °C.
- 2) CTAB and CTAC surfactants are C₁₆ alkyl chain length surfactants whereas DTAB and DTAC C₁₂ alkyl chain length surfactants. The CTAC and CTAB surfactants exhibited higher foamability when combined with APG surfactants owing to the increased adsorption energy. Decreased surface adsorption and reduced hydrophobicity could be the main governing reasons for the APG surfactant having higher foamability as compared to the APG/DTAB and APG/DTAC surfactant formulations.
- 3) The stand-alone APG surfactant solution obtained the lowest interfacial tension value at 1.79 mN/m. Addition of cationic surfactants increased the surface and interfacial tension of the surfactant formulation containing APG surfactant. The lack of charge on the surfactant head facilitated lower surface and interfacial tension values for the non-ionic (APG) surfactant as compared to cationic surfactants (CTAB, CTAC, DTAB and DTAC).
- 4) The incremental oil recovery obtained for pure CO₂, APG/CTAC and APG/CTAB foam flooding was 18.5%, 24.5% and 32.7%, respectively and the estimated carbon storage potential for pure CO₂, APG/CTAC and APG/CTAB foam flooding was 11.9%, 15.8% and 23.7%, respectively. The differential pressure response of the APG/CTAC and APG/CTAB surfactant formulations were similar. Although both of the surfactant formulations showed higher differential pressure, the higher oil recovery and carbon storage potential of APG/CTAB surfactant formulations can be attributed to the wettability alteration from oil-wet to water-wet, caused by the more effective counter-ion effect: Br⁻ vs. Cl⁻.

For future work, exploring the effect of crude oil and variation in the formation brine salinity on the bulk foam and coreflooding experiments is warranted as it shall further reflect the foamability and foam stability of the APG and cationic surfactant formulations at the actual reservoir conditions. Moreover, the addition of polymers to further enhance the stability of the surfactant formulation is worth estimating for high pressure and temperature reservoir conditions.

Acknowledgements

The authors acknowledge the Indian Institute of Technology, Kharagpur, University of Bergen, and NFiP (Petroleum Research School of Norway), Norway for providing infrastructural and monetary support. The authors also acknowledge the Research Council of Norway and the industry partners of NCS2030 RCN project number 331644 for their support.

Conflict of interest

The authors declare no competing interest.

Open Access This article is distributed under the terms and conditions of the Creative Commons Attribution (CC BY-NC-ND) license, which permits unrestricted use, distribution, and reproduction in any medium, provided the original work is properly cited.

References

- Adebayo, A. R. Sequential storage and in-situ tracking of gas in geological formations by a systematic and cyclic foam injection-A useful application for mitigating leakage risk during gas injection. *Journal of Natural Gas Science and Engineering*, 2019, 62: 1-12.
- Alcorn, Z. P., Fredriksen, S. B., Sharma, M., et al. An integrated CO₂ foam EOR pilot program with combined CCUS in an onshore Texas heterogeneous carbonate field. Paper SPE 190204 Presented at the SPE Improved Oil Recovery Conference, Tulsa, Oklahoma, 14-18 April, 2018.
- Bello, A., Ivanova, A., Cheremisin, A. Enhancing N₂ and CO₂ foam stability by surfactants and nanoparticles at high temperature and various salinities. *Journal of Petroleum Science and Engineering*, 2022, 215: 110720.
- Chai, J., Cui, X., Zhang, X., et al. Adsorption equilibrium and dynamic surface tension of alkyl polyglucosides and their mixed surfactant systems with CTAB and SDS in the surface of aqueous solutions. *Journal of Molecular Liquids*, 2018, 264: 442-450.
- Chen, S., Han, M., AlSofi, A., et al. Non-ionic surfactant formulation with ultra-low interfacial tension at high-temperature and high-salinity conditions. Paper SPE 200273 Presented at the SPE Conference at Oman Petroleum & Energy Show, Muscat, Oman, 21-23 March, 2022.
- Daerr, A., Mogne, A. Pendent_drop: An imagej plugin to measure the surface tension from an image of a pendent drop. *Journal of Open Research Software*, 2016, 4(1): e3.
- de Azevedo, B. R. S., Alvarenga, B. G., Percebom, A. M., et al. Interplay of interfacial and rheological properties on drainage reduction in CO₂ foam stabilised by surfactant-

- t/nanoparticle mixtures in brine. *Colloids and Interfaces*, 2023, 7(1): 2.
- Ding, L., Jouenne, S., Gharbi, O., et al. An experimental investigation of the foam enhanced oil recovery process for a dual porosity and heterogeneous carbonate reservoir under strongly oil-wet condition. *Fuel*, 2022, 313: 122684.
- Gao, M., Lei, F., Liu, Q., et al. The effect of alkyl chain length in quaternary ammonium cationic surfactants on their foaming properties. *Russian Journal of Physical Chemistry A*, 2019, 93: 2735-2743.
- Hou, J., Lin, S., Du, J., et al. Study of the adsorption behavior of surfactants on carbonate surface by experiment and molecular dynamics simulation. *Frontiers in Chemistry*, 2022, 10: 847986.
- Jian, G., Alcorn, Z., Zhang, L., et al. Evaluation of a nonionic surfactant foam for CO₂ mobility control in a heterogeneous carbonate reservoir. *SPE Journal*, 2020, 25(6): 3481-3493.
- Kian, K., Scurto, A. M. Viscosity of compressed CO₂-saturated n-alkanes: CO₂/n-hexane, CO₂/n-decane, and CO₂/n-tetradecane. *The Journal of Supercritical Fluids*, 2018, 133: 411-420.
- Kutschmann, E. M., Findenegg, G. H., Nickel, D., et al. Interfacial tension of alkylglucosides in different APG/oil/water systems. *Colloid and Polymer Science*, 1995, 273: 565-571.
- Li, F., Yu, X., Fang, H., et al. Influence of polymerization degree on the dynamic interfacial properties and foaming ability of ammonium polyphosphate (APP)-surfactant mixtures. *Journal of Molecular Liquids*, 2021, 335: 116175.
- Ma, J., Li, L., Wang, H., et al. Carbon capture and storage: History and the road ahead. *Engineering*, 2022, 14: 33-43.
- Ma, L., Zhu, M., Liu, T. Effects of chain length of surfactants and their adsorption on nanoparticles on stability of CO₂-in-water emulsions. *Colloids and Surfaces A: Physicochemical and Engineering Aspects*, 2022, 644: 128877.
- Massarweh, O., Abushaikha, A. S. Application of surfactants in enhancing oil recovery from tight carbonates: Physicochemical properties and core flooding experiments. *Geoenery Science and Engineering*, 2023, 221: 211400.
- Mohamed, A., Trickett, K., Chin, S. Y., et al. Universal surfactant for water, oils, and CO₂. *Langmuir*, 2010, 26(17): 13861-13866.
- Onyebuchi, V. E., Kolios, A., Hanak, D. P., et al. A systematic review of key challenges of CO₂ transport via pipelines. *Renewable and Sustainable Energy Reviews*, 2018, 81: 2563-2583.
- Pang, J., Mohanty, K. Increase of CO₂ storage in high-salinity carbonate reservoirs by foam injection. Paper SPE 214951 Presented at the SPE Annual Technical Conference and Exhibition, San Antonio, Texas, USA, 16-18 October, 2023.
- Para, G., Jarek, E., Warszynski, P. The Hofmeister series effect in adsorption of cationic surfactants-theoretical description and experimental results. *Advances in Colloid and Interface Science*, 2006, 122(1-3): 39-55.
- Patist, A., Oh, S. G., Leung, R., et al. Kinetics of micellization: Its significance to technological processes. *Colloids and Surfaces A: Physicochemical and Engineering Aspects*, 2001, 176(1): 3-16.
- Petkova, B., Tcholakova, S., Cherkova, M., et al. Foamability of aqueous solutions: Role of surfactant type and concentration. *Advances in Colloid and Interface Science*, 2020, 276: 102084.
- Rafati, R., Technology, U., Hamidi, H. Application of sustainable foaming agents to control the mobility of carbon dioxide in enhanced oil recovery. Paper SPE 163287 Presented at the SPE Kuwait International Petroleum Conference and Exhibition, Kuwait City, Kuwait, 10-12 December, 2012.
- Razavi, S. M. H., Shahmardan, M. M., Nazari, M., et al. Experimental study of the effects of surfactant material and hydrocarbon agent on foam stability with the approach of enhanced oil recovery. *Colloids and Surfaces A: Physicochemical and Engineering Aspects*, 2020, 585: 124047.
- Rezaee, M., Hosseini-Nasab, S. M., Fahimpour, J., et al. New insight on improving foam stability and foam flooding using fly-ash in the presence of crude oil. *Journal of Petroleum Science and Engineering*, 2022, 214: 110534.
- Sæle, A., Graue, A., Alcorn, Z. P. Unsteady-state CO₂ foam injection for increasing enhanced oil recovery and carbon storage potential. *Advances in Geo-Energy Research*, 2022, 6(6): 472-481.
- Sanders, A. W., Jones, R. M., Linroth, M., et al. Implementation of a CO₂ foam pilot study in the SACROC field: Performance evaluation. Paper SPE 160016 Presented at the SPE Annual Technical Conference and Exhibition, San Antonio, Texas, USA, 8-10 October, 2012.
- Santa, M., Alvarez-Jürgenson, G., Busch, S., et al. Sustainable surfactants in enhanced oil recovery. Paper SPE 145039 Presented at the SPE Enhanced Oil Recovery Conference, Kuala Lumpur, Malaysia, 19-20 July, 2011.
- Thakore, V., Ren, F., Voytek, J., et al. High temperature stability of aqueous foams for potential application in enhanced geothermal system (EGS). Paper Presented at the 45th Workshop on Geothermal Reservoir Engineering Stanford University, Stanford, California, 10-12 February, 2021.
- Wang, J., Xue, G., Tian, B., et al. Interaction between surfactants and SiO₂ nanoparticles in multiphase foam and its plugging ability. *Energy & Fuels*, 2017a, 31(1): 408-417.
- Wang, Y., Zhang, Y., Liu, Y., et al. The stability study of CO₂ foams at high pressure and high temperature. *Journal of Petroleum Science and Engineering*, 2017b, 154: 234-243.
- Wei, P., Pu, W., Sun, L., et al. Alkyl Polyglucosides stabilized foam for gas controlling in high-temperature and high-salinity environments. *Journal of Industrial and Engineering Chemistry*, 2018, 60: 143-150.
- Wei, P., Zhai, K., Guo, K., et al. Highly viscous liquid foam for oil-displacement: Surface & phase behavior enhance-

- ment. *Journal of Petroleum Science and Engineering*, 2022, 212: 110274.
- Wei, Y., Kang, J., Liu, L., et al. A proposed global layout of carbon capture and storage in line with a 2 °C climate target. *Nature Climate Change*, 2021, 11(2): 112-118.
- Wen, Y., Yu, T., Xu, L., et al. Molecular dynamics and experimental study of the effect of pressure on CO₂ foam stability and its effect on the sequestration capacity of CO₂ in saline aquifer. *Chemical Engineering Science*, 2024a, 284: 119518.
- Wen, Y., Zhong, Y., Zeng, P., et al. Interfacial chemical mechanisms of brine salinity affecting the CO₂ foam stability and its effect on the sequestration capacity of CO₂ in deep saline aquifer. *Journal of Molecular Liquids*, 2024b, 399: 124349.
- Wu, X., Xiao, P., Liu, B., et al. Experimental investigation on using CO₂/H₂O emulsion with high water cut in enhanced oil recovery. *Petroleum Science*, 2024, 21(2): 974-986.
- Wu, X., Zhang, Y., Zhang, K., et al. An experimental investigation of liquid CO₂-in-water emulsions for improving oil recovery. *Fuel*, 2021, 288: 119734.
- Xiao, B., Ye, Z., Wang, J., et al. Law and mechanism study on salt resistance of nonionic surfactant (alkyl glycoside) foam. *Energies*, 2022, 15(20): 7684.
- Yekeen, N., Padmanabhan, E., Idris, A. K. Synergistic effects of nanoparticles and surfactants on n-decane-water interfacial tension and bulk foam stability at high temperature. *Journal of Petroleum Science and Engineering*, 2019, 179: 814-830.
- Yu, Y., Hanamertani, A. S., Ahmed, S., et al. Supercritical CO₂-foam screening and performance evaluation for CO₂ storage improvement in sandstone and carbonate formations. Paper SPE 208141 Presented at the Abu Dhabi International Petroleum Exhibition & Conference, Abu Dhabi, UAE, 15-18 November, 2021.
- Zhang, C., Geng, T., Jiang, Y., et al. Impact of NaCl concentration on equilibrium and dynamic surface adsorption of cationic surfactants in aqueous solution. *Journal of Molecular Liquids*, 2017, 238: 423-429.
- Zhang, C., Xue, Y., Huang, D., et al. Design and Fabrication of anionic/cationic surfactant foams stabilized by lignin-cellulose nanofibrils for enhanced oil recovery. *Energy & Fuels*, 2020, 34(12): 16493-16501.